Journal of Materials and Environmental Sciences
ISSN : 2028-2508
CODEN : JMESCN

J. Mater. Environ. Sci., 2018, Volume 9, Issue 11, Page 3075-3086

http://www.jmaterenvironsci.com

Experimental and quantum chemical studies on ethanol extract of *Phyllanthus amarus* (EEPA) as a green corrosion inhibitor for aluminium in 1 M HCl

[1]Nnbuk Okon Eddy and [2]Femi Awe Emmanuel and [3]Emeka Ogoko

[1]*Department of Chemistry, Federal University, Lokoja, Kogi State, Nigeria*
[2]*Department of Chemistry, Federal University, Dutsinma, Katsina State, Nigeria*
[3] *Department of Chemistry, National Open University of Nigeria, Abuja, Nigeria*

Received 05 Nov 2017,
Revised 31 Mar 2018,
Accepted 04 Apr 2018

Keywords
- ✓ Corrosion,
- ✓ Aluminium,
- ✓ Inhibition,
- ✓ *Phyllanthus amarus*.

nabukeddy@yahoo.com
Phone: +2348038198753

Abstract

Ethanol extract of *Phyllanthus amarus* (EEPA) is investigated as a possible green corrosion inhibitor for aluminium in solution of HCl. Weight loss, linear and potentiodynamic polarization methods were used to evaluate the inhibition efficiencies of various concentrations of the plant extract. Scanning electron microscopy and Fourier transformed infra red spectroscopy were used to study the surface morphology and engagement of functional groups in the inhibition process. The results obtained at 303 K from weight loss, linear polarization resistance and potentiodynamic polarization methods recorded inhibition efficiencies that ranged from 56.65 to 69.17, 65.00 to 93.93 and from 51.38 to 79.96 % respectively. Generally, inhibition efficiency decreases with increase in concentration but increased with a rise in temperature. Potentiodynamic study, reveals that EEPA acted as a mixed type inhibitor and formed a protective film, which protected the metal against corrosion. Examination of micrographs in the presence and absence of the inhibitor, indicated the formation of a protective film that blocks the active corrosion sites on the surface of the metal. Also, analysis of spectra obtained from Fourier transformed infra red study indicated that EEPA was adsorbed unto the surface of aluminium via C=O and OH functional groups. The adsorption of the inhibitor was spontaneous, exothermic and supported the mechanism of physical adsorption. Calculated quantum chemical parameters for the chemical constituents of EEPA revealed that phyllanthusin D is the most active corrosion inhibitor in the compound. The HOMO and LUMO diagrams of Phyllanthusin D supported the findings from FTIR analysis.

1. Introduction

Corrosion is an electrochemical process that degrades and converts metals to their natural state. The effect of such destruction is enormous because of the high cost required for the replacement of damaged metallic components. Aluminium is one of the most industrial valuable metals. Therefore protecting the metal against major destruction (which may be primarily due to corrosion) is necessary. Although several protection/control measures against corrosion are available, the use of corrosion inhibitors is one of the best and acceptable options[1]. Corrosion inhibitors are substances that retard the rate of corrosion of a metal, when added in a minute concentration [2]. Trends in research, development and application of corrosion inhibitors in industries have moved from inorganic inhibitors to organic inhibitors and to green inhibitors in recent times [3]. Extracts of plants are widely accepted as components that have promising feautures in the corrosion industries [4]. This is because most of them are cheap, easily available, biodegradable and eco-friendly [5]. The present study is designed to investagate the corrosion inhibition properties of ethanol extract of *Phyllanthus amarus* (EEPA) for aluminium in 1 M HCl.

Phyllanthus amarus is generaly regarded as a weed, although some of its medicanal values have been harnessed in recent times [6]. Good success has been widely recorded on the potency of this plant extract as a corrosion inhibitor for some metals. For example, Okafor *et al*. [7], found that seeds, leaves and a combination

of seeds and leaves extracts of *Phyllanthus amarus* are good adsorption corrosion inhibitors for mild steel in HCl and H_2SO_4 solutions. The extracts inhibited the corrosion of mid steel through the mechanism of chemical adsorption. Their adsorption best fitted the Temkin adsorption model. Sangeetha *et al*. [8], also found that a combination of *Phyllanthis amarus* extract with Zn^{2+} system in the ratio of 2 ml : 25 ppm yeided inhibition efficiency of 98 % for the corrosion of carbon steel in aqeuous solution containing 60 ppm of chloride solution. Polarization data revealed that the *Phyllanthus amarus* extract acted as a mixed type inhibitor while AC impedance data indicated the formation of a protective film that formed a barrier against further corrosion attack. However, in their study, they did not provide data that could enable the mechanism of adsorption and the best fitted adsorption isotherms to be proposed. Pasupathy *et al*. [9], also investigated the corrosion inhibition efficiency of leaves extract of *Phyllanthus amarus* for zinc in 0. 5 N H_2SO_4 and found that the extract is a good adsorption inhibitor for zinc. Althogh the authors did not investigate the mechanism of adsorption of the inhibitor, they were able to found that the adsorption of the extract obeyed the Temkin adsorption model. Sribharahy *et al*. [10], found that extract of *Phyllanthus amarus* inhibited the corrosion of mild steel in sea water, with maximum inhibition effieicncy approaching 98 %. The extract, however acted as an anodic inhibitor for mild steel in sea water. Olusegun and Otaigbe [11] studied the corosion inhibition potential of extract from *Phyllanthus amarus* and found that the extract was a good adsorption inhibitor for the corrosion of aluminium in alkaline solution. Maximum inhibition efficiency of 76 % was recorded and the adsorption characteristics of the inhibitor responded best to the Langmuir adsorption model. Although the authors did not investigate the effect of temperature and were unable to propose the mechanism of adsorption of the extract on the surface of the metal, a zero order kinetics were proposed by them. Eddy [6] used ethanol extract of *Phyllanthus amarus* to inhibit the corrosion of mild steel in solution of H_2SO_4 and found that the extract acted as an adsorption inhibitor for mild steel corrosion. However, he proposed a physiosorption mechanism, whose adsorption characteristics fitted the Langmuir adsorption model.

From the above review, it is indicative that the mode of adsorption, mechanism of inhibition and adsorption characteristics of *Phylanthus amarus* as a corrosion inhibitor vary with the type of metal, type of aggresive medium and the mode of extraction. To the best of our knowledge, literature on the use of phyllanthus amarus as an inhibitor for aluminium in solution of HCl is scanty. The present study is aimed at using ethanol extract of *Phylanthus amarus* to inhibit the corrosion of aluminium in 1 M HCl solution

2. Materials and method

Aluminium sheet was obtained from the department of metallurgy, Ahmadu Bello University. Analar grade of concentrated hydrochloric acid was purchased from Sigma Aldrich Chemical company and double distilled water was used for the preparation of the test solution (i.e 1 M HCl). Samples of *Phyllanthus amarus* leaves were obtained from the Ahmadu Bello University Botanical garden. The leaves were dried, grounded to powdered form and soaked in ethanol. Cold extraction was carried out in order to obtained the ethanol soluble extract. The extract obtained, was used to prepared a stock solution of EEPA, from where 0.1, 0.2, 0.3, 0.4 and 0.5 g/L concentrations of the extract were obtained through serial dilution.

2.1 Weight loss experiment.

Weight loss experiment was carried out by immersing a 5 x 4 cm aluminium coupon in the respective test solution (1 M HCl and 0.1, 0.2, 0.3, 0.4 and 0.5 g/L of EEPA in 1 M HCl respectively) contained in a 250 ml beaker. It was ensured in all cases that the test solution sufficiently covered the metal, After every 24 hours, each coupon was withdrawn from the solution, washed in distilled water, dried and weighed. The experiments were repeated untill 168 hours of immersion. Values of weight loss obtained after every 24 hours of immersion were recorded. From weight loss data, the inhibition efficiency of EEPA was calculated using equation 1:

$$\%IE = \frac{weight\ loss}{initial\ weight} \times \frac{100}{1} \qquad 1$$

The degree of surface coverage was obtained by dividing the inhibition efficiency by 100 while the corrosion rate of aluminium was obtained using equation 2:

$$CR\ (gcm^{-2}h^{-1}) = \frac{weight\ loss}{Area\ of\ the\ metal\ coupon \times period\ of\ immersion} \qquad 2$$

2.2 Polarization study

Linear polarization resistance (LP) measurements were carried out using a potentiostat (model: AuT71791 and PGSTAT 30). The potential range of -1000 to 2000 mV and at a scan rate of 0.33 mV/s at 303 K were used. . Each test was run in triplicate. All measurements were done in an autolab frequency response

analyser coupled to a potentiostat, connected to a computer system. The working electrode was the aluminium metal of 1 cm^2 area, the counter electrode was a platinum electrode in a glass corrosion cell kit, the reference electrode was a Ag/Ag system and the experiment was carried out with the working electrode immersed in 1 M HCl under static condition.

For PDP measurements, the corrosion rate of the inhibitor was calculated through corrosion current density l_{corr}, which was obtained by extrapolating the linear Tafel segments of the anodic and cathodic curves. Also, the inhibition efficiency (I%) was calculated using equation 6 [12]:

$$\%I = \frac{i^0_{Corr} - i_{Corr}}{i^0_{Corr}} \times \frac{100}{1} \qquad 3$$

However, for LPR, the over potential and current data was plotted on a linear scale to get LPR plots, and the slope of the plots in the vicinity of the corrosion potential gave the polarisation resistance (R_p). From the measured values of R_p, the inhibition efficiency (I %) was calculated using the following equation [12]:

$$\%I = \frac{R_{p(Inh)} - R_p}{R_{p(Inh)}} \times \frac{100}{1} \qquad 4$$

where R_p and $R_{p(inh)}$ are the uninhibited and inhibited polarization resistance, respectively

2.3 Quantum chemical alculations

All chemical structures were drawn using the Chem draw package in the ChemBio2015 Cambridge software. Geometry optimization was performed with hyperchem release 10 software. Hyperchem release 10 software was also used to calculate the molecular energies of the compounds using PM3 Hamiltonian. The HOMO and LUMO diagrams were developed using the Chem 3D programme in the package in the ChemBio2015 Cambridge software. All calculations were carried out on gas phase state of the molecules.

3. Results and discussions

3.1 Weight loss

Weight loss of mild steel, taken after every 24 hours immersion in the test solution was used to developed graphs of variation of weight loss with time and to estimate the relative values of the corrosion rate of aluminium in the test solution. Figure 1 shows plots of variation of weight loss with time for the corrosion of aluminium in 1 M HCl solution containing various concentrations of ethanol extract of *Phyllanhus amarus* (ERPA) at 303 K.

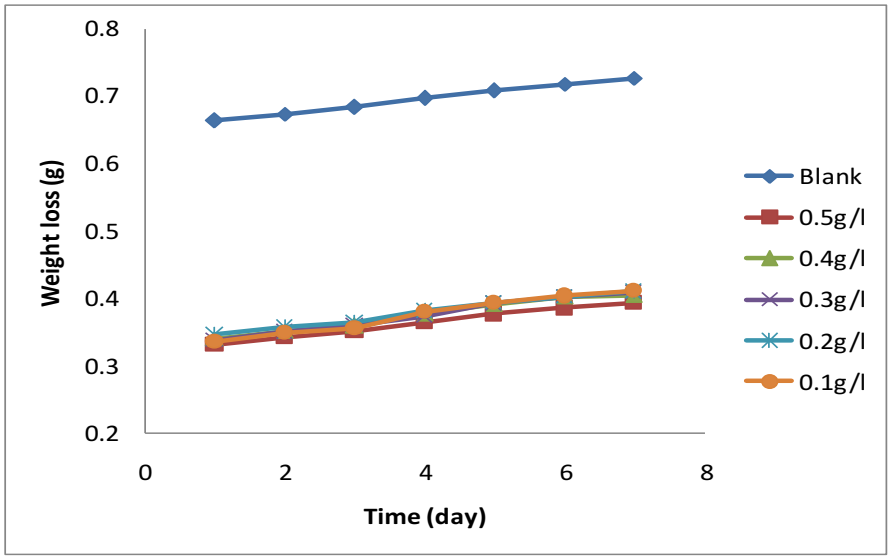

Figure 1: Variation of weight loss with time for the corrosion of aluminium in 0.1 M HCl containing various concentrations of EEPA

Graphs obtained at 313, 323 and 333 K are not shown but the corrosion rates at 303 K and these temperatures are presented in Table 1. Geenerally, weight loss of mild steel was found to increase with increase in the period of contact and with increasing temperture. Addition of EEPA decreases the weight loss of aluminium in 1 M HCl such that weight loss decreases with increase in the concntration of EEPA. An increase in weight loss corresponded to increase in corrosion rate and vice versa. Therefore, EEPA decreases the corrosion rate of

aluminium in 1 M HCl, which indicates that EEPA inhibited the corrosion of aluminium in 1 M HCl. The inhibition efficiency of the extract (EEPA) increases with concentration but decreased with a rise in temperature as shown in Table 1. It is an established fact that from the pattern of variation of inhibition efficiency with temperature, the mechanism of adsorption can be proposed.

Table 1: Corrosion rate of aluminium in solutions of HCl and inhibition efficiency of EEPA for Al

	CR (g/h/cm^2)				%I			
C (g/L)	**303K**	**313K**	**323 K**	**333 K**	**303K**	**313K**	**323 K**	**333 K**
Blank	0.00355	0.005206	0.010417	0.016861				
0.1	0.001539	0.002722	0.007233	0.012433	56.65	47.71	30.56	26.26
0.2	0.001256	0.002489	0.006672	0.011222	64.63	52.19	35.95	33.44
0.3	0.0012	0.002367	0.006544	0.010867	66.20	54.54	37.17	35.55
0.4	0.001106	0.002383	0.006356	0.010633	68.86	54.22	38.99	36.94
0.5	0.001094	0.002111	0.006033	0.010044	69.17	59.45	42.08	40.43

Decrease in inhibition efficiency with increasing temperature points toward physiosorption mechanism while an increase in inhibition efficiency with temperature defines a chemisorption mechanism. Therefore the adsorption of EEPA on aluminium surface favours the mechanism of physical adsorption [13] .

3.2 Polarization study

Data obtained from linear polarization (LPR) and potentiodynamic polarization (PDP) are presented in Table 2. Under LPR study, the inhibition efficiency of EEPA was also found to increase with concentration and ranged from 65.00 to 93.93 %, which is higher than the range of 56.65 to 69.17 % obtained from weight loss measurements. Therefore, the instantaneous inhibition potential of EEPA is better than its average inhibition potential.

Table 2: Polarization data and inhibition efficiencies of various concentrations of EEPA for the corrosion of Al in HCl

C (g/L)	**PDP**						**LPR**	
	β_a	**β_b**	**E_{corr}(V)**	**I_{Corr} (A)**	**CR (mm/y)**	**%I**	**R_p (Ω)**	**%I**
Blank	0.16516	0.076753	-0.92637	0.000494	5.3597		46.087	
0.1	0.6669	0.081721	-1.2171	0.000240	2.6058	51.38	131.69	65.00
0.2	0.38349	0.68213	-1.1110	-1.109500	2.0371	61.99	568.03	91.89
0.3	0.10458	0.084662	-1.2103	0.000151	1.6397	69.41	134.51	65.74
0.4	1.2355	0.037523	-1.2155	0.000132	1.4333	73.26	119.77	61.52
0.5	-0.19327	0.091313	-1.2551	0.000099	1.0741	79.96	759.63	93.93

Inhibition efficiencies obtained for various concentrations of EEPA from PDP measurements ranged from 51.38 to 79.96 %. This range also reveals that, for similar concentration of the extract, the inhibition efficiencies obtained from PDP measurements are relatively higher than those obtained from weight loss measurements but less than those obtained from LPR measurement. PDP plots for various concentrations of EEPA is presented in Figure 2. In the presence of the inhibitor, the cathodic and anodic Tafel slopes are less or more equal suggesting that EEPA acted as a mixed type inhibitor. It is evident from the plots that the transition from active zone to passivating zone as the corrosion potential increases to the passivation potential (Epp) proves the formation of pasivating film, Mixed type inhibitors are generally known as corrosion inhibitors that form protective film, which may be a precipitate that blocks the corrosion active sites of the anode and the cathode in order to protect the metal against further corrosion attack [14]. However, it is generally believed that when the difference between the corrosion potential of the blank and that of the system containing the inhibitor is above 85 mV, then the the inhibitor can be classified as cathodic (Eddy *et al*.,2015). In this study, the differences for 0.1, 0.2, 0.3, 0.4 and 0.5 g/L of EEPA were 291, 185, 284, 290 and 329 mV respectively. Therefore, in addition to EEPA being a mixed type inhibitor, cathodic behaviour contributes dominatly to its inhibitory behaviour.

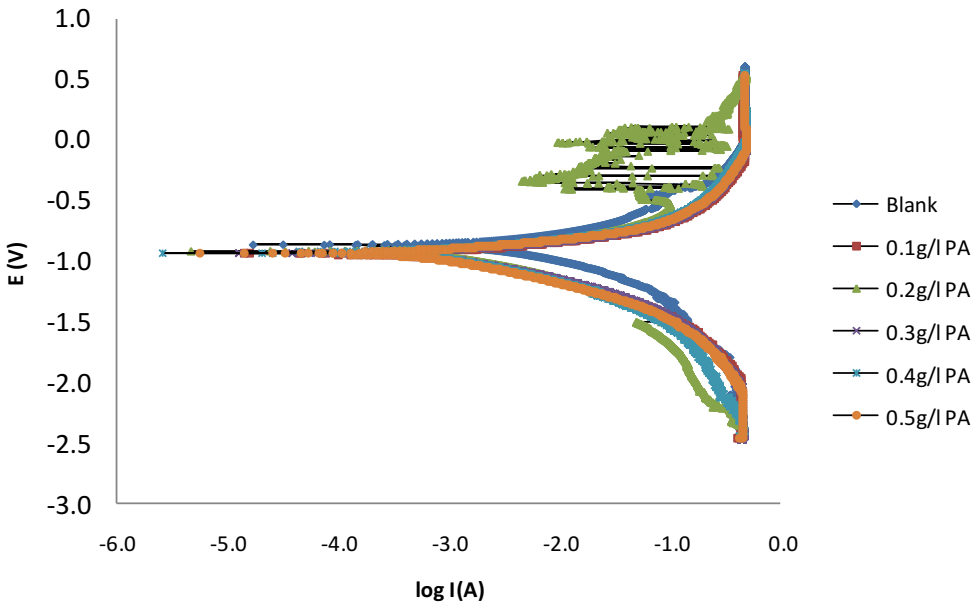

Figure 2: Potentiodynamic plot for the corrosion of aluminium in 1 M HCl containing various concentrations of EEPA

3.3 Effect of temperature

The Arrhenius equation is most suitable for use in estimating the minimum energy requirement for the corrosion and inhibition of the corrosion of aluminium in solutions of HCl. The model relates the corrosion rate to the activation energy according to equation 5 [15],

$$CR = Aexp\left(\frac{-E_a}{RT}\right) \qquad 5$$

where CR is the corrosion rate, A is the Arrhenius or pre-exponential factor, E_a is the activation energy, R is the gas constant and T is the temperature. Equation 5 was applied by taking the natural logarithm of both sides to obtain equation 6,

$$\ln(CR) = \ln(A) - \frac{E_a}{RT} \qquad 6$$

Since equation 9 is a linear model, a plot of ln(CR) versus 1/T was found to give straight line, whose slope and intercept are $\frac{E_a}{R}$ and ln(A) respectively. This plot is shown in Figure 3 and the various parameters deduced from the plots are recorded in Table 3. Values of R^2 calculated from the plots were very close to unity, confrming a high degree of linearity and the application of the Arrhenius model to the present data. From the results presented in Table 3, the activation energy for the blank was 44.62 J/mol.

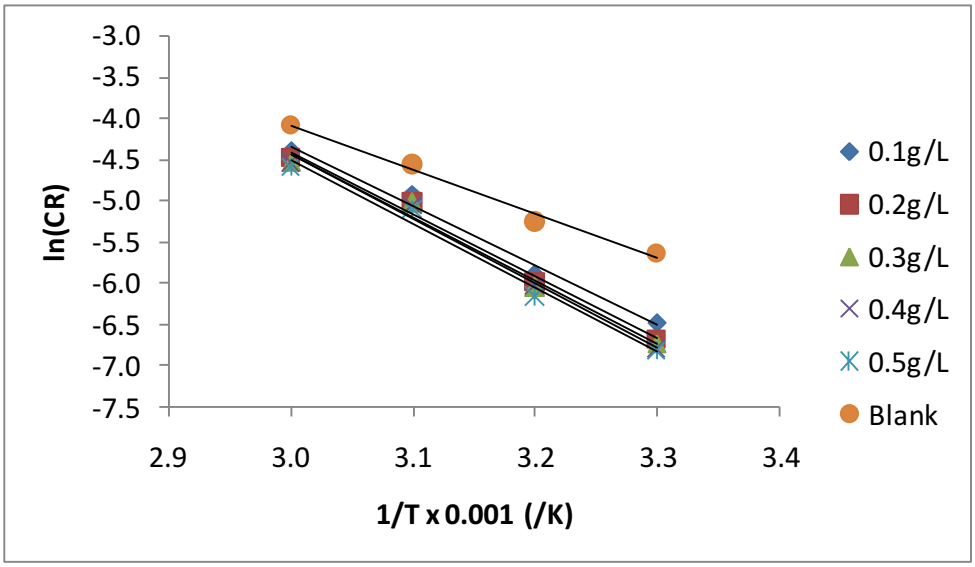

Figure 3: Arrhenius plot for the corrosion of aluminium in 1M HCl containing various concentrations of EEPA

Table 3: Arrhenius and Transition state adsorption parameters for the corrosion of aluminium in 1 M HCl containing various concentration of EEPA

C (g/L)	Arrhenius parameters			Transition state parameters				
	ln(A)	E_a (J/mol)	R^2	slope	intercept	ΔS^0_{ads} (J/mol)	ΔH^0_{ads} (J/mol)	R^2
Blank	12.02	44.62	0.988	5.053	5.209	-41.33	-42.01	0.987
0.1	17.39	60.23	0.986	6.93	10.64	3.82	-57.62	0.985
0.2	18.25	62.81	0.987	7.241	11.5	10.97	-60.20	0.986
0.3	18.44	63.41	0.985	7.312	11.69	12.55	-60.79	0.984
0.4	18.86	64.66	0.987	7.456	12.11	16.05	-61.99	0.986
0.5	18.58	64.03	0.983	7.386	11.83	13.72	-61.41	0.982

In the presence of various concentrations of EEPA, the activation energy, which ranged from 60.23 to 64.03 J/mol progressively increases with concenration of the extract, indicating that the adsorption becomes more thermodynamically stable with increasing concentration of the inhibitor. Generally, activation energy below 80 kJ/mol points toward physical adsorption mechanism while those above 80 kJ/mol are associated with chemisorption mechanism [16]. Therefore, it is indicative that the adsorption of EEPA on the surface of aluminium operates through the mechanism of physical adsorption.

Table 3 also reveals that the Arhenius or pre-exponential constant ranged from 17.39 to 18.58 as against the value of 12.02, recorded for the blank. Although the significance of the constant is not well known, an equillibration between the Arhenius and the Transition state equation, reveals that it is associated with entropy.

3.4 Thermodynamic/adsorption study

In adsorption, thermodynamic parameters of interest are the entropy of adsorption, enthalpy of adsorption and the standard free energy of adsorption. The Transition state equation was used to estimate the entropy and enthalpy of adsorption of EEPA on the surface of aluminium. The logarithm form of the Transition state equation, which relates the corrosion rate with temperature can be expressed acording to equation 7 [17],

$$ln\left(\frac{CR}{T}\right) = ln\left(\frac{R}{Nh}\right) + \left(\frac{\Delta S^*_{ads}}{R}\right) - \frac{\Delta H^*_{ads}}{RT} \qquad 7$$

N is the Avogadro's number, h is the Planck constant, ΔS^*_{ads} is the standard change in entropy and ΔH^*_{ads} is the standard enthalpy change. In accordance with the mathematical implication of equation 7, plotting of values of $ln\left(\frac{CR}{T}\right)$ against 1/T gave straight lines (Figure4) with excellent (approximating 100 %) degree of linearity.

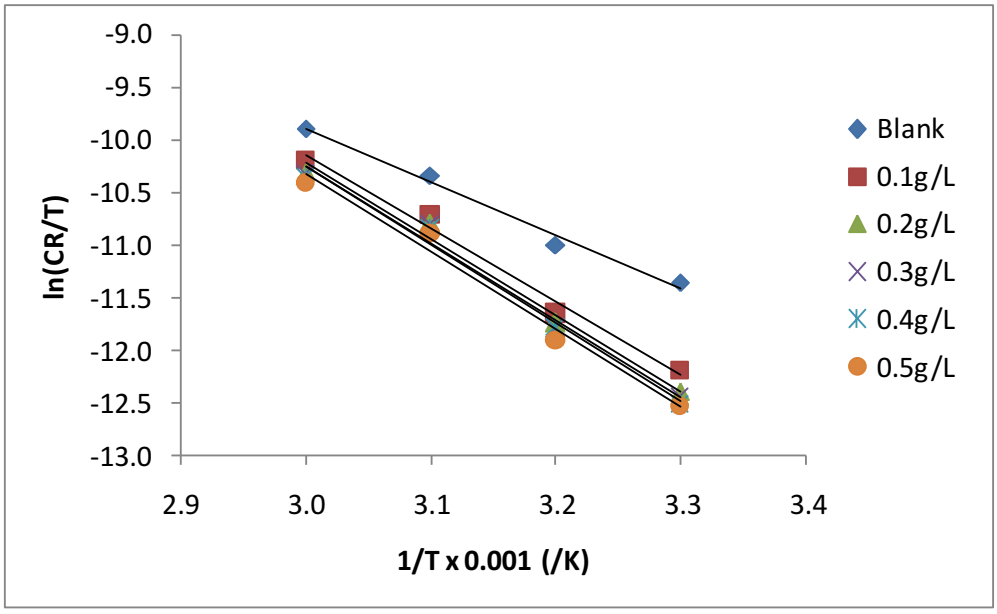

Figure 4: Transition state plot for the corrosion of aluminium in solution of HCl at various concentrations of **EEPA**

Values of standard changes in entropy and enthalpy calculated from the intercepts and slopes of the plots were recorded in Table 3. The entropy change for the blank was -41.33 J/mol but in the presence of various concentrations of EEPA, the change in entropy ranged from 3.82 to 13.72 J/mol. However, changes in enthalpy ranged from -57.62 to -61.99 J/mol in the presence of various concentrations of EEPA but -42.01 J/mol for the blank. Positive values of entropy change suggests disorderliness while negatie values of enthalpy change indicate that the reaction is exothermic. However a spontaneous adsorption will be defined when ΔS^*_{ads} is positive and ΔH^*_{ads} is negative or when $\Delta H^*_{ads} < T\Delta S^*_{ads}$. Within the confinement of the range of temperature considered in this work, there is no doubt that the calculated values of changes in entropy and enthalpy will favour spontaneous adsorption of EEPA unto aluminium surface. Low values obtained for both thrmodynamic parameters are consistent with the mechanism of physical adsorption.

In corrosion inhibition, adsorption is the initial mechanism for any inhibition process. Although there are two basic types of adsorption, differences exist between the adsorption characteristics of different inhibitors. The response of a given inhibitor to an established adsorption model provides information on the mode of adsorption and on the adsorption characteristies. In search for the best fitted adsorption isotherm for the studied inhibitor, different adsorption isotherms were tested and the tests indicated that the best fitted adsorption isotherm is the Langmuir and Frendlich adsorption isotherm. The Langmuirs adsorption isotherm can be expressed as follows [18].,

$$ln\left(\frac{C}{\theta}\right) = lnC - lnb_{ads} \qquad 8$$

where C is the concentration of EEPA in the bulk electrolyte, θ is the degree of surface coverge of EEPA and b_{ads} is the equilibrium constant of adsorption. Langmuir isotherm for the adsorption of EEPA is shown in Figure 5 while Table 4 contains values of adsorption parameters of EEPA, calculated from the Langmuir isotherms. The fitness of the data to the Langmuir adsorption model is sustained by excellent degree of linearity (R^2 ranged from 0.996 to 0.998). Values of the equilibrium constant of adsorption was found to decrease with increase in temperature, which indicate that the strength of adsorption decreases with temperature and is typical for physiosorption mechanism. However, slope values deviated from ideal value of unity but ranged from 0.748 to 0.880. The basic assumptions of the Langmuir equation include the the absence of interaction between the adsorbed molecules and homogenousity of all adsorption sites, which translates to the independency of the free energy of adsortion on the surface site and on the surface coverage. The non unity slope values obtained in this work suggest that these conditions are not made by the adsorption of EEPA on the surface of aluminium. The existence of interaction between adsorbed molecules, as indicated by the non unity slope values, may be due to lateral interaction existing in the molecules, when they get closer to each other. Therefore, they may be sites with different free energy of adsorption.

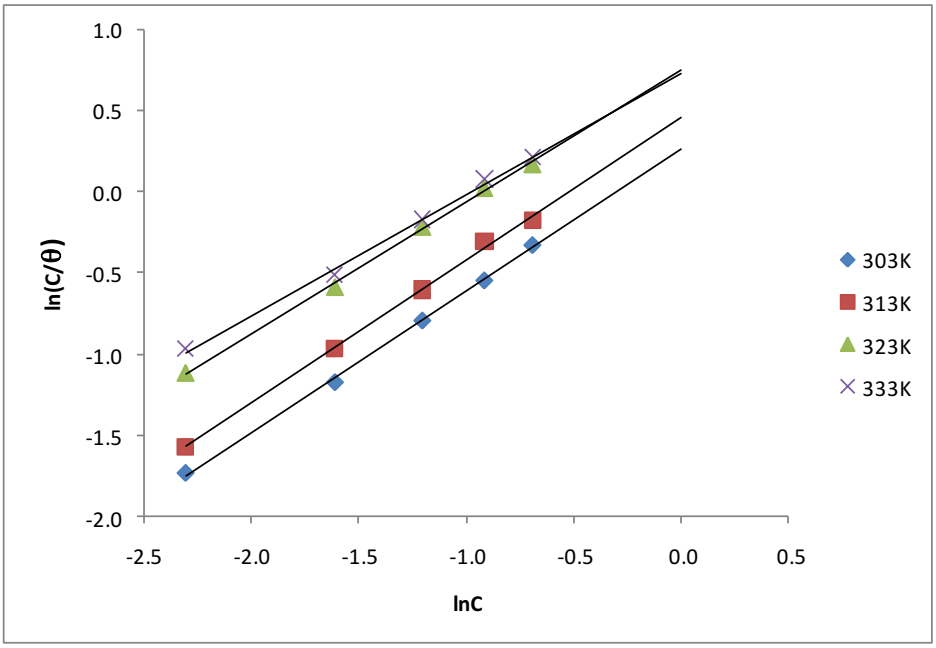

Figure 5: Langmuir isotherm for the adsorption of EEPA on the surface of aluminium

The assumptions establishing the Freundlich adsorption model can be written as [19],

$$ln\theta = lnb_{ads} + \frac{1}{n} lnC \qquad 9$$

where θ is the degree of surface coverage, b_{ads} is the adsorption equillibrium constant b_{ads} and n are Freundlich constants. b_{ads} is related to adsorption capacity. The higher the adsorption capacity, the higher the value of b_{ads}. On the other hand, 1/n is a measure of the intensity of the adsorption. The higher the value of 1/n, the more favourable is the adsorption. Generally, n<1 and 1/n > 1. Figure 6 shows the Freundlich isotherm for the adsorption of EEPA on the surface of mild steel. From the results of Freundlich adsorption parameters presented in Table 4, it is evident that values of 1/n and b_{ads} increase with increase in temperature, which suggest that the adsorption becomes more stabilized as the temperature increases.

Thermodynamic direction of a chemical reaction and the mechanism of adsorption can be predicted through the sign and magnitude of standard free energy change. Generally, negative values of standard free energy change points toward spontaneous reaction and values of standard free energy of adsorption upto – 20 kJ/mol or less negative, reflects physiosorption mechanism. In this study, values of standard free energy change were calculated by substituting b_{ads} values obtained from Langmuir and Freundlich isotherms into the following equation [20],

$$b_{ads} = -\frac{1}{55.5} exp \frac{\Delta G^0_{ads}}{RT} \qquad 10$$

Values of standard free energy of adsorption calculated from both options, are recorded in Table 4. These values ranged from -9.45 to -8.27 J/mol and from -19.78 to -11.97 J/mol respectively. Therefore, the adsorption of EEPA is spontaneous and favours the mechanism of physical adsorption [21].

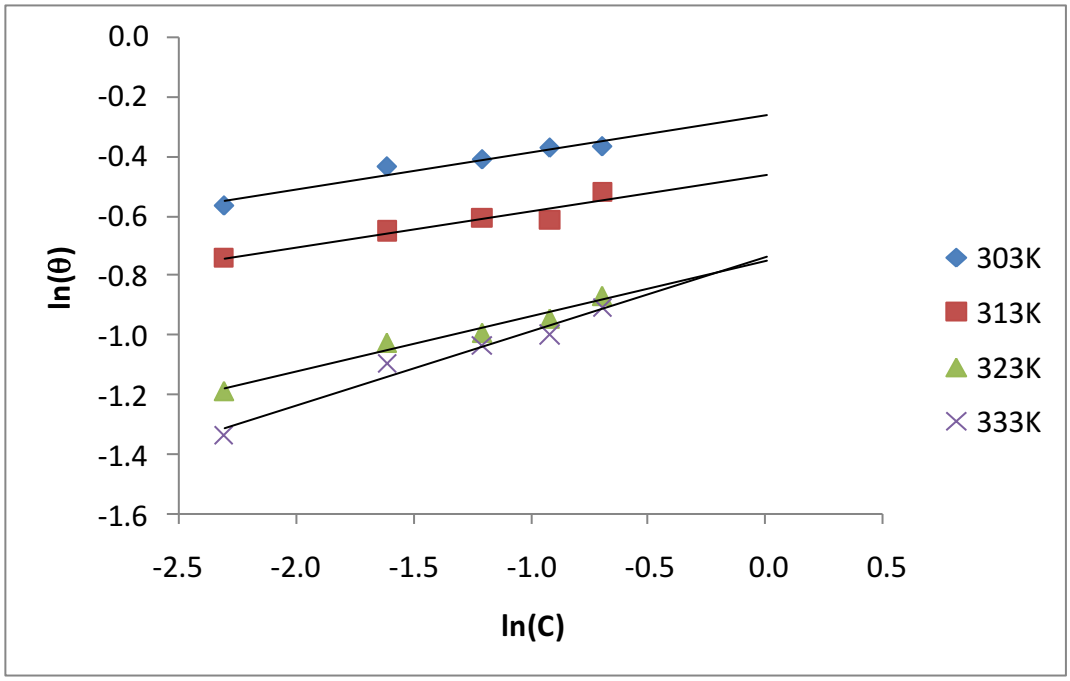

Figure 6: Freundlich isotherm for the adsorption of EEPA on the surface of aluminium

Table 4: Langmuir and Freundlich parameters for the adsorption of EEPA on the surface of aluminium

T (K)	Langmuir				Freundlich			
	slope	lnb_{ads}	ΔG^0_{ads} (J/mol)	R^2	n	lnb_{ads}	ΔG^0_{ads} (J/mol)	R^2
303 K	0.875	-0.264	-9.45	0.998	0.125	0.264	-10.78	0.945
313K	0.880	-0.464	-8.95	0.998	0.125	0.464	-11.29	0.911
323K	0.815	-0.753	-8.22	0.998	0.200	0.753	-12.0	0.971
333K	0.748	-0.735	-8.27	0.996	0.250	0.735	-11.97	0.967

3.5 Scanning electron microscopy (SEM)

The SEM micrograph of the corroded surface of aluminium drawn out from the test solution of HCl is presented in Figure 7a. When 0.5 g/L of EEPA was used as an inhibitor, the micrograph obtained is also shown in Figure 7b. It is evident from the micrographs that in the absence of an inhibitor, the corrosion is seen to penetrates the metal deeply, whereas, in the presence of EEPA, the surface of the metal is covered by a protective layer. Therefore, EEPA formed a protective layer on the surface of aluminium, in order to prevent further corrosion attack.

3.6 Fourier transformed infra red (FTIR) spectroscopy

Frequencies of IR adsorption deduced from FTIR spectra of EEPA and the corrosion product of aluminium (when EEPA was used as an inhibitor) are presented in Table 5. Major functional groups associated with the various bonds in EEPA are =C-H stretch, C-O stretch, N-H stretch, C=O stretch and OH stretch. Interactions of the inhibitor with the surface of the metal remarkably shifted the =C-H bend from 759 to 853 cm^{-1}, the C-O stretch from 1050 to 1092 cm^{-1}, another C-O stretch was shifted from 1210 to 1209 ccm^{-1}, C-C stretch from 1442 to 1443 cm^{-1}, N-H bend from 1616 to 1614 cm^{-1} and OH stretch from 3416 to 3414 cm^{-1}. However, C=O stretch and OH which appeared on the spectrum of the EEPA at 1722 and 2935 cm^{-1} respectively, were missing. Therefore, EEPA was adsorbed to the surface of aluminium through these functional groups.

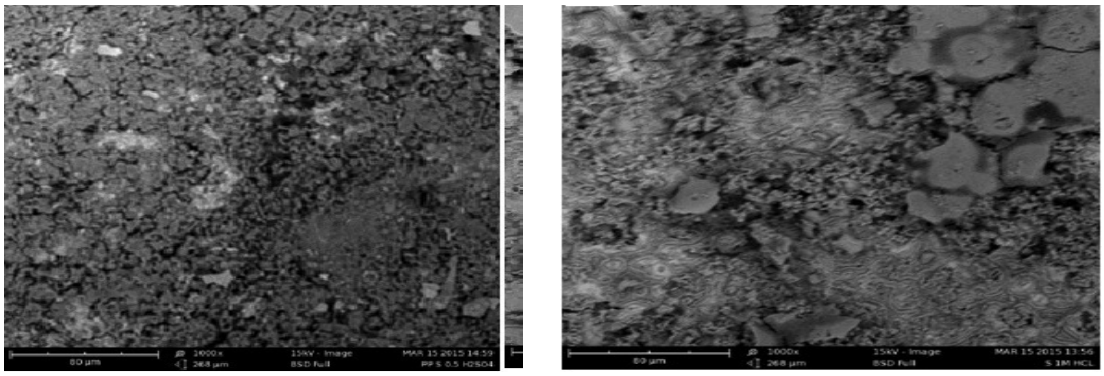

(a) (b)

Figure 7: Scanning electron micrograph of the corrosion product of mild steel in the (a) absence & presence of 0.5 g/L EEPA

Table 5: Peaks, frequencies and assignment of IR absorption by EEPA and the corrosion product of mild steel in the presence of EEPA

0.5 g/L EEPA			**Corrosion Product + 0.5 g/L EEPA**		
Frequency of IR	**Area**	**Assignment**	**Frequency of IR**	**Area**	**Assignment**
759.01	55.71	=C-H Bend	853.53	53.64	=C-H Bend
1050.28	199.48	C-O Stretch	1091.75	91.33	C-O Stretch
1210.37	94.66	C-O Stretch	1209.41	49.57	C-O Stretch
1441.84	89.52	C-C stretch in ring	1442.8	98.72	C-C stretch (in ring)
1616.40	71.77	N-H bend	1613.51	164.17	N-H bend
1721.53	125.97	C=O Stretch	-	-	-
2934.79	790.05	O-H Stretch	-	-	-
3416.05	624.96	O-H Stretch	3414.12	881.09	O-H Stretch

*3.7 Active constituents of EEPA and their adsorption properties*Major chemical constituents of EEPA are phyllanthusin D, phyllanthin, hypophyllanthin, quercetin, amarin, 1,2,8-trimethyl-7-vinylnaphthalene, etc, [8-9]). The chemical structures of these compounds are shown in Figure 8. As a rule, most organic corrosion inhibitors are compounds that have hetero atoms in aromatic ring or long carbon chain. In addition, availability of conjugated system, suitable functional groups and π-electrons are additional features that can effectively enhance the corrosion inhibition efficiencies of organic inhibitors [22]. A careful examination of the chemical structures of major constituents of EEPA (i.e Figure 8) convincinly reveals that EEPA has compounds that meet these conditions. Therefore, its inhibition properties can be alligned to its chemical constituents. A classical inspection of the chemical structures of these compounds can not in any way furnishes information on the

preffered compounds that are responsible for corrosion inhibition or provide an order for their increasing inhibition efficiency. According to Eddy *et al*. [23], quantum chemical indices, especially, the frontier molecular orbital energies can be used to effectively sort the compounds in order of their increasing or decreasing inhibition efficiency

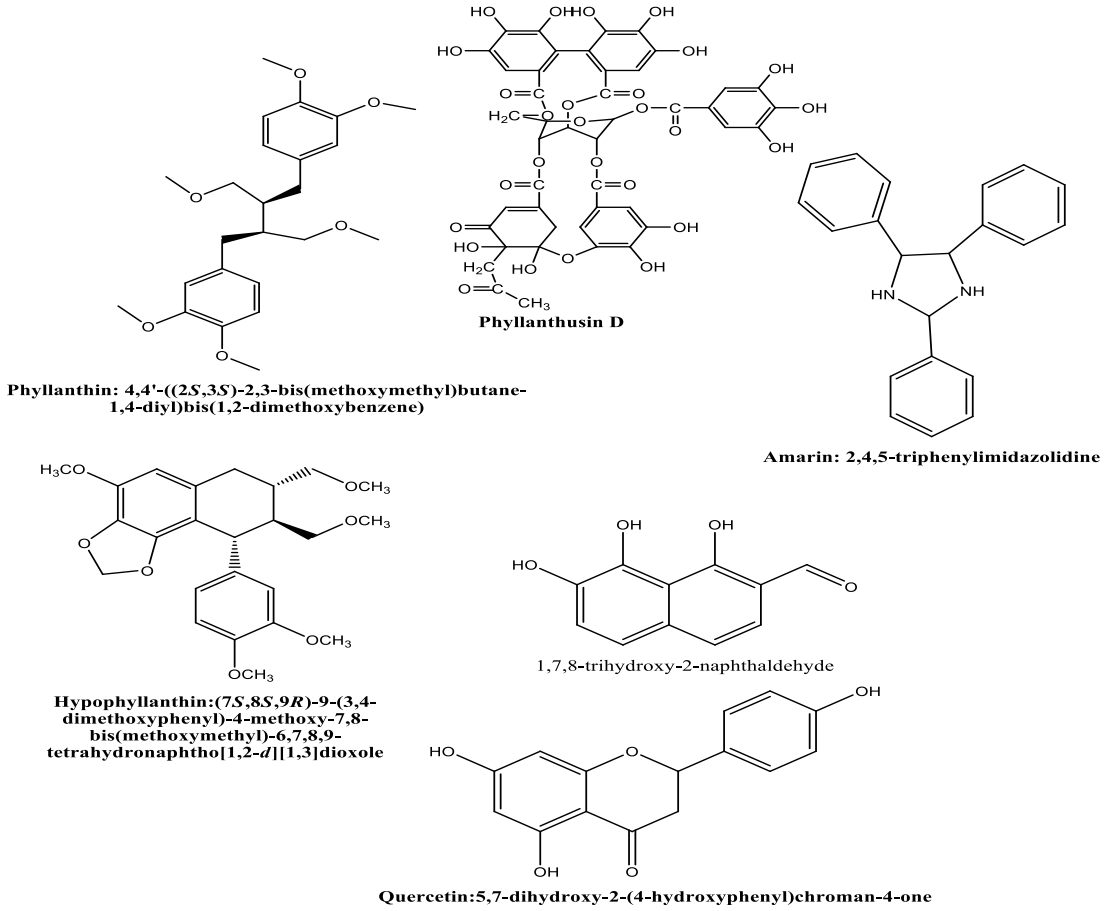

Figure 8: Chemical structures of major component of EEPA

3.8 Quantum chemical study

Table 6 presents calculated values of molecular energies of molecules in EEPA. The calculated energies include the frontier molecular energies (i.e the energy of the highest occupied molecular orbital (E_{HOMO}), the energy of the lowest unoccupied molecular orbital (E_{LUMO}) and the energy gap (E_{L-H} or ΔE), the electronic energy of the molecules (E_{Elect}), the binding energy of the molecules (E_b) and the core- core repulsion eergy (E_{CCR}).

Table 6: Molecular energies of chemical constituents of EEPA

	E_{HOMO} (eV)	E_{LUMO} (eV)	ΔE (eV)	E_b (eV)	E_{elect} (eV)	E_{CCR} (eV)
phyllanthusin D	-8.991	-1.477	7.515	-13185.71	-182580.92	168887.19
phyllanthin	-8.713	0.388	9.101	-277.24	-47714.94	42574.78
hypophyllanthin	-8.912	0.380	9.292	-271.33	-49559.28	44187.35
quercetin	-9.615	-0.634	8.981	-156.38	-22234.13	18797.03
amarin	-9.411	0.143	9.554	-205.41	-25771.90	22646.24
1,2,8-trimethyl-7-vinylnaphthalene	-8.684	-0.935	7.750	-112.90	-2492.07	12143.42

From the point of view of corrosion inhibition, the E_{HOMO} represent the tendency of a chemical specie to donate electron or charge, indicating that the higher the value of E_{HOMO}, the better the inhibition efficiency is expected

[24]. On the other hand, the E_{LUMO} is an index that correspond to the tendency of a chemical specie to accept electron or charge during a reaction, therefore, better corrosion inhibitor should be characterised with low values of E_{LUMO} [25]. The differences between E_{LUMO} and E_{HOMO} define the energy gap of a molecule. Based on the energy gap, molecules may be classified as hard or soft. Soft molecules are more reactive than hard molecules because they have a lower energy gap, indicating that the energy needed for an electron to move from the HOMO level to the LUMO level will be minimal compare to that of hard molecules. The more an inhibitor presents itself with easy provision for transition from the HOMO to the LUMO level, the better is the expected efficiency. Therefore, soft molecules are expected to exhibit better inhibition efficiency than hard molecule.

Based on the value of E_{HOMO}, contributions of the constituents of EEPA to its inhibition efficiency for the corrosion of aluminium is expected to be consistent with the following order, 1,2,8-trimethyl-7-vinylnaphthalene > phyllanthin >hypophylanthin> phyllanthusin D>amarin>quercetin. However, based on the respective values of E_{LUMO}, the expected order should be, phyllanthin D > 1,2,8-trimethyl-7-vinylnaphthalene > quercetin > amarin > hypophyllanthin > phyllanthin but based on the enery gap, which is described as the difference between E_{LUMO} and E_{HOMO}, the expected trend is pyllanthusin > 1,2,8-trimethyl-7-vinylnaphthalene > quercetin > phyllanthin > hypophyllanthin > amarin. The binding enrgy of a molecule represent the energy that is holding the molecule together. This means the higher the binding energy, the more difficult it would take the molecule to go into reaction. Consequently, based on the E_b of the molecules in EEPA, the relative contribution to corrosion inhibition should be phyllanthusin D > phyllanthin > hypophyllanthin > amarin > quercetin > 1,2,8-trimethyl-7-vinylnaphthalene. Similarly, the higher the energy possess by electrons, the better should the inhibition efficiency be expected. Consequently, the expected trend for the variation of inhibition efficiency, based on the E_{electr} is phyllanthusin D > hypophyllanthin > phyllanthin > amarin > 1,2,8-trimethyl-7-vinylnaphthalene > quercetin. Finally, core core repusion energy is expected to increase with inhibition efficiency and the expected trend is phyllanthusin D > hypophyllanthin > phyllanthin > amarin > quercetin > 1,2,8-trimethyl-7-vinylnaphthalene.

From the above analysis, it is evident that phylanthusin D is the major contributor to the corrosion inhibition potential of EEPA. However, this does not imply that the other constituents does not contributes significantly. It is necessary to state that a system such as EEPA, where there are different corrosion active components, the overall inhibition efficiency is a consequence of synergistic adsorption of the various active components in the inhibitor. It is also interesting to state that all the molecular energies calculated for the various constituents of EEPA are within the range of values expected for good corrosion inhibitors.

In Figure9, the HOMO and LUMO diagram of phyllanthusin D is shown. It is interesting to note that while the positive and negatives lobes of the phyllanthusin D HOMO diagram is resting on the biphenyl-2,2',3,3',4,4'-hexaol end of the molecule, those of the LUMO is concentrated on the 5,5,6-trihydroxy-6-(2-oxopropyl)cyclohex-2-enone end of the molecule.

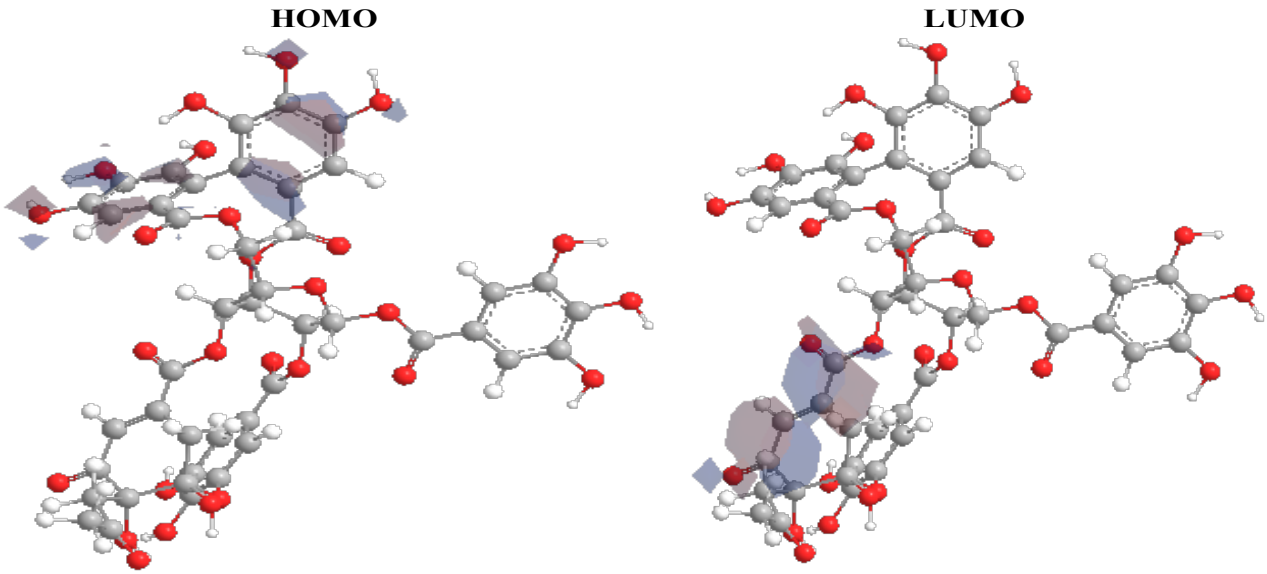

Figure9: HOMO and LUMO diagrams of phyllanthusin D

This implies that biphenyl-2,2',3,3',4,4'-hexaol end, which has several hydroxyl bonds will be the electron or charge donating sites. The molecular orbital diagrams support the finding from FTIR results that hydroxyl and carboxyl groups are essential for the adsorption of EEPA on the surface of the molecule.

Conclusion

The present study was aimed at investigating the corrosion inhibition properties of EEPA for aluminium in solution of HCl and to examine the major components that are responsible for its inhibitive action. The study reveals that EEPA is a good adsorption inhibitor that is capable of inhibiting the corrosion of aluminium in 1 M HCl, to a large extent. However, the instantaneous inhibition potential of the extract is better than its average inhibition efficiency. EEPA acted as a mixed type corrosion inhibitor, exhibiting the strength of blocking active corrosion sites of the metal surface through the formation of protective film. The mechanism of adsorption of the inhibitor is consistent with physiosorption. The adsorption of the inhibitor on the surface of aluminium is spontaneous and its characteristics allign excellently with the Langmuir and the Freundlich adsorption models.

References

1. A. S. Founda, A. A. Al-Sarawy, F. Sh-Ahmed, H. M. El-Abbasy. *Corros. Sci.* 51(1)(2009) 485.
2. A. A. Maayta, N. A. F. El Rawashdeh, *Corros. Sci.* 46(5)(2004) 1129.
3. N. O. Eddy, U. J. Ibok, P. O. Ameh, N. O. Alobi, M. M. Sambo, *Chem. Engr. Comm.* 201(10)(2014) 1360.
4. B. E. Amitha-Rani, B. B. J Basu, *Intern. J. Corros*. 2012: http://dx.doi.org:10.1155/2012/380217.
5. J. Bushweishaija, *Tanz. J. Sci.* 35 (2009) 77.
6 N. O. Eddy, *Portugaliae Electrochimica Acta* 27(5)(2009) 579.
7. P.C. Okafor, M.E. Ikpi, I.E. Uwah, E.E. Ebenso, U.J. Ekpe, S.A. Umoren, *Corros. Sci.* 50(8)(2008) 2310.
8. M. Sangeetha, S. Rajendran, J. Sathiyabama, A. Krishnaveni, N. Manimaran, B. Shyamaladevi, *Electrochimica Acta* 29(6) (2011) 429.
9. A. Pasupathy, S. Nirmala, G. Abirami, A. Satish, R.P. Milton, *Intern. J. Scient. Res Pub.* 4(3)(2014) 1.
10. V. Sribharathy, S. Rajendran, J. Sathiyabama, *Chem. Sci. Trans.* 2(1)(2013) 315.
11. K. A. Olusegun, J. O. E. Otaigbe, *Corros. Sci.* 51(2009) 2790.
12. P. O. Ameh, N. O. Eddy, *Cogent Chem.* 2 (2016) 1253904.
13. E. El ouariachi, A. Bouyanzer, R. Salghi, B. Hammouti, J. M. Desjobert, J. Costa, J. Paolini, L. Majidi, *Research on Chemical Intermediates* 41(2)(2015) 935.
14. M. Finsgar, J. Jackson, *Corrosion Science* 86 (2014)17.
15. N. Chaubey, V. K. Singh, M. A. Quraishi, E. E. Ebenso, *Intern. J. Electrochem. Sci.*10(2015) 504.
16. B.M. Prasanna, B.M. Praveen, N. Hebbar, T.V. Venkatesha, H.C. Tandon, *Intern. J. Indust. Chem.* 7(1) (2016) 9.
17. A. Singh, V. K. Singh, M. A. Quraishi, *Arabian J. Sci. Engr.* 38(1)(2013) 85.
18. H. L. Wang, H. Fan, J. Zhang, *Mater. Chem. Phys.* 72(3)(2003) 655.
19. A. A. Khadom, A. S. Yaro, A. A. H. Kadhum, *J. Chilean Che, Soc.* 1(2010) 150.
20. S.A. Umoren, M.J. Banera, T. Alonso-Garcia, C.A. Gervasi, M.V. Mirifico, *Cellulose* 20(5)(2013) 2529.
21. K. O. Orubite, N.C. Oforka, *Mater. Letts.* 58(11)(2004). 1768- 1772.
22. N. Raghavendra, I. Bhat, *J. Chem. intermediate* 42(2016) 6351. Doi.10.1007/s11164-016-2467-1.
23. N. O. Eddy, H. Momoh-Yahaya, E. E. Oguzie, *J. Adv. Res*. 6(2015) 203.
24. N. O. Eddy, B. I. Ita, *Intern. J. Quant. Chem.* 111(14)(2011)3456.
25. N. O. Eddy, B. I. Ita, *J. Mol. Mod.* 17(2011) 633.